energies

MDPI

Article

Experimental Performance Evaluation of a PV-Powered Center-Pivot Irrigation System for a Three-Year Operation Period

Juan Ignacio Herraiz [1,2], Rita Hogan Almeida [1], Manuel Castillo-Cagigal [2] and Luis Narvarte [1,*]

[1] Instituto de Energía Solar–Universidad Politécnica de Madrid, C/Nicola Tesla s/n, 28031 Madrid, Spain; ji.herraiz@upm.es (J.I.H.); rita.hogan@upm.es (R.H.A.)
[2] Qualifying Photovoltaics, C/Alan Turing 1, 28031 Madrid, Spain; m.castillo@qpv.es
* Correspondence: luis.narvarte@upm.es

Abstract: High-power diesel-based or grid-connected irrigation systems are being replaced by battery-free, high-power stand-alone Photovoltaic Irrigation Systems (PVIS) that reduce energy costs by up to 80% and for which no experimental performance data are available. The operation of PVIS is affected by various factors, some unrelated to the quality of the PV system itself, that generate losses that affect their performance: losses that vary with the crop and its irrigation period, losses intrinsic to the PVIS design, and losses that happen as a consequence of the behavior of the end-user. To better understand the impact of each type of loss, the traditional performance ratio was factorized. This paper provides the PV community with experimental data on the performance of a battery-free 160 kWp PV-powered constant-pressure center-pivot irrigation system. The system was analyzed over three years of real operation, during which the performance ratio ranged from 49.0 to 53.2%.

Keywords: water pumping system; PV irrigation system; performance; stand-alone PV system

Citation: Herraiz, J.I.; Almeida, R.H.; Castillo-Cagigal, M.; Narvarte, L. Experimental Performance Evaluation of a PV-Powered Center-Pivot Irrigation System for a Three-Year Operation Period. *Energies* **2023**, *16*, 3654. https://doi.org/10.3390/en16093654

Academic Editors: Frede Blaabjerg, Vladimir Prakht, Anton Rassõlkin, Levon Gevorkov, Emiliia Iakovleva and Irina Kirpichnikova

Received: 23 March 2023
Revised: 17 April 2023
Accepted: 21 April 2023
Published: 24 April 2023

1. Introduction

Stand-alone photovoltaic (PV) pumping systems have been present in the world since the 1970s, when Dominique Campana coordinated the installation of the first PV water pumping system in Corsica, France [1]. Father Bernard Vespieren, director of the non-governmental organization "Mali Aqua Viva" in Mali and one of the first visitors to the Corsica pumping system, introduced the first PV pump in Africa in 1977 [2].

Although these first experiences used ad hoc DC drivers to couple the pumps to the PV generators, innovations like the one presented by [3] allowed the use of standard frequency converters to feed standard AC centrifugal pumps. The power of these stand-alone PV pumping systems was limited to a few tens of kW due to the intermittent character of solar irradiance until five years ago, as can be seen in research from that period [4]. Sudden variations in irradiance caused by shadows from passing clouds made it impossible to ensure the stability of the FC of high-power PV pumping systems and led to control instabilities and sudden stops of the FC, producing water hammers in the hydraulic system and over-voltages between the FC output and the motor pump.

Despite this, these relatively small-power pumping systems have been widely used throughout the world for various applications, such as human drinking water supply [5], water supplies for livestock [6], or irrigation of crops [7,8].

They have also attracted the attention of researchers, who have investigated various technical aspects related to the optimization of their design based on the simulation of different systems like direct pumping [9], drip irrigation [10,11], multi-pumping [12,13], floating PV systems [14], and methodological aspects [15]. Other studies have been related to their control, such as the tuning of the PID control of the frequency converter [16], the application of artificial intelligence to the prediction of their productivity [17,18], the

assessment of their performance [19,20] or its prediction [21], the development of different sizing methods [22,23] or simulation tools [24], the integration of storage [25], or the technical feasibility in different regions [26,27].

The economic viability of these pumping systems has also been researched. For example, in [28], the authors evaluated the socio-economic and climatic impact of PV drip and sprinkler irrigation systems, reporting savings of up to 66% in kWh cost. Others have explored the best ways to finance them, such as [29], presenting solutions based on blockchain technology to produce financial instruments suited to attracting investors to PV pumping projects. Others have explored the policy frameworks that may favor the implementation of irrigation systems [30]. Others have assessed PV pumping systems as a tool to reduce the environmental impact of agriculture [31].

The rising energy costs of modernized agriculture in the last few years have increased the need to expand the power of PV pumping systems for large-scale irrigation. The innovations developed in the framework of a European project [32], solving problems associated with PV power intermittences without the need for batteries [33], allowed the implementation of stand-alone high-power photovoltaic irrigation systems (PVIS) [34] that are not only economically feasible but also environmentally sustainable [35]. An alternative solution was the integration of batteries [36], but it was found to not be economically feasible for high power applications.

Prior work on performance has been focused on grid-connected PV systems, where performance basically depends on the quality of the system itself. Experience in its calculation and a deep knowledge of the experimental values of the most used performance indices, such as the Performance Ratio (*PR*), exist in the literature [37]. There are also experimental performance data for small power PV irrigation systems, such as those reported by [19] (monthly *PR* values between 59.7% and 93.1%). In the case of high-power PVIS, there is a lack of experimental data on their performance in the literature. Furthermore, the operation of high-power PVIS is limited by external factors other than their quality, and, therefore, the use of performance indices like the *PR* needs to be reconsidered. In order to quantify and better understand the impact of these external factors on performance, in 2018, Almeida et al. [34] proposed factorizing the traditional *PR* into various utilization ratios. The new indices considered different types of losses: losses strictly related to the PV system itself (PR_{PV}); losses that vary with the crop and the irrigation period (UR_{IP}); those intrinsic to the design of the PV generator and the hydraulic infrastructure (UR_{PVIS}); and losses that occur as a consequence of the behavior of the irrigator (UR_{EF}) [34].

However, given the recent market introduction of PVIS, there are still very few publications reporting experimental *PR* values and even fewer on the values of the indices resulting from *PR* factorization. So far, data have only been published for two PVIS pumping to water pools (at variable pressure and water flow) [38], and no data are known for PVIS pumping at a constant flow and pressure, like the ones using pivots for irrigation. The characteristics of constant flow and pressure, in which the working frequency and the power consumed by the pump are constant, point to a *PR* lower than that of PVIS pumping to a water pool, but this has not been experimentally proven.

In order to address the limitations of prior work on the experimental performance of high-power PVIS, this paper provides experimental performance data for a PV-powered center-pivot PVIS working at a constant-pressure over a three-year period, adding to the knowledge of the expected performance of this kind of system. Experimental data are crucial since knowing the expected performance values is key to establishing quality thresholds in technical specifications and quality control procedures in the context of contractual frameworks for the sale and installation of high-power PVIS. Additionally, in this paper, the performance was evaluated both under stable irradiance conditions and also under conditions of fluctuating PV power from 2019 to 2022, quantifying the different utilization factors relevant to assessing the effect of external factors on the performance of high-power PVIS.

The paper is structured as follows: after the introduction, the materials and methods section describes the PVIS under study, the performance indices to be calculated, and the way the data were filtered and processed. Section 3 presents the results of the performance evaluation. Section 4 discusses the results, and Section 5 summarizes the conclusions obtained and proposes some future lines of research.

2. Materials and Methods

2.1. Description of the PVIS under Study

2.1.1. The Pre-Existing Irrigation System

The irrigation system (IS) was located in Alaejos, Spain (41°16′23.4″ N, 5°16′48.8″ E) and belonged to the cooperative "Estrella de San Juan". It is used to irrigate a total area of 88 ha.

Figure 1 presents the pre-existing IS, which consisted of a diesel generator feeding two frequency converters. Each FC fed one of two pumps: a 92 kW submersible pump (Caprari–E10S50S/6C + MAC10125DS-8V), pumping water from a 140 m deep borehole to an elevated water tank of 1000 m^3, and a 30 kW surface centrifugal pump (Caprari–MEC-AS2/80A + FELM 30KW 2P), pumping water from the tank to the irrigation network at the constant-pressures required by a set of four pivots.

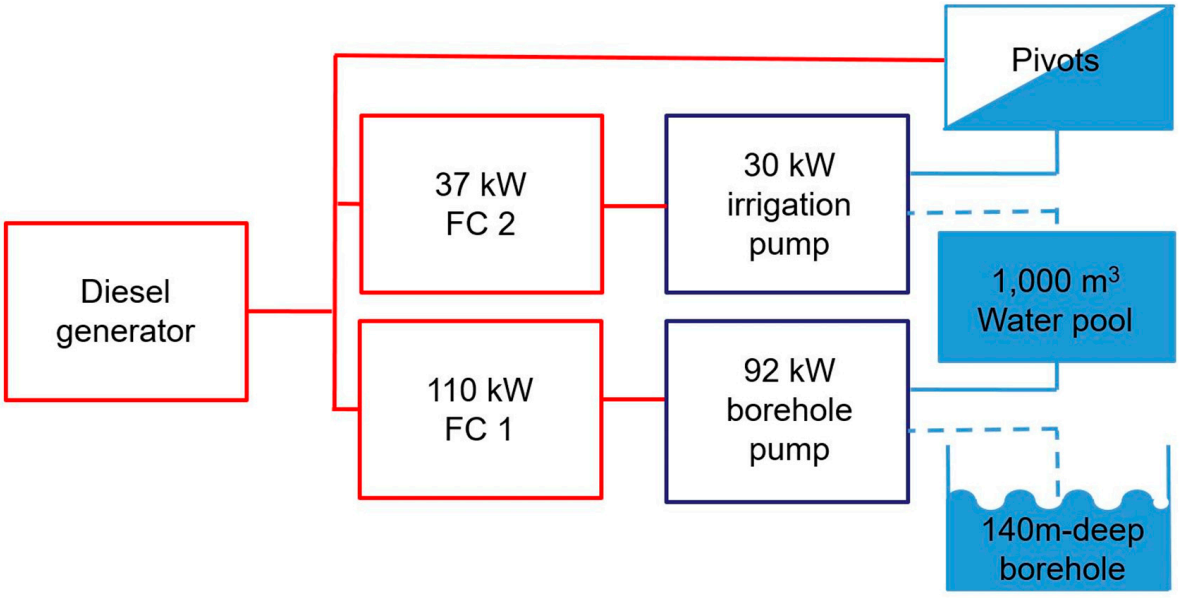

Figure 1. Pre-existing IS configuration: The diesel generator feeds the borehole, irrigation pumps, and the pivots.

2.1.2. The New PVIS

The new PVIS consisted of a 160 kWp PV generator, divided into eight North–South horizontal trackers, and three additional FCs: a 110 kW FC that fed the 92 kW submersible pump (hereinafter, "pumping FC"), a 37 kW FC that fed the 30 kW pump (hereinafter, "irrigation FC"), and another 37 kW FC used to feed the motors that move the pivots and work at a constant frequency of 50 Hz to simulate an electrical grid (hereinafter, "pivots FC"). The motors that drive the pivots are always on during irrigation. Their average consumption is 4.5 kW, but current peaks occur when the motors start and stop. The pivots FC is oversized to withstand these peaks. After the PVIS commissioning, the actual power of the PV generator was measured at 150.3 kWp. Figure 2 shows the configuration of the PVIS. Even though it was designed to replace the previous one, it was decided to keep the diesel generator and the old IS for greater irrigator confidence.

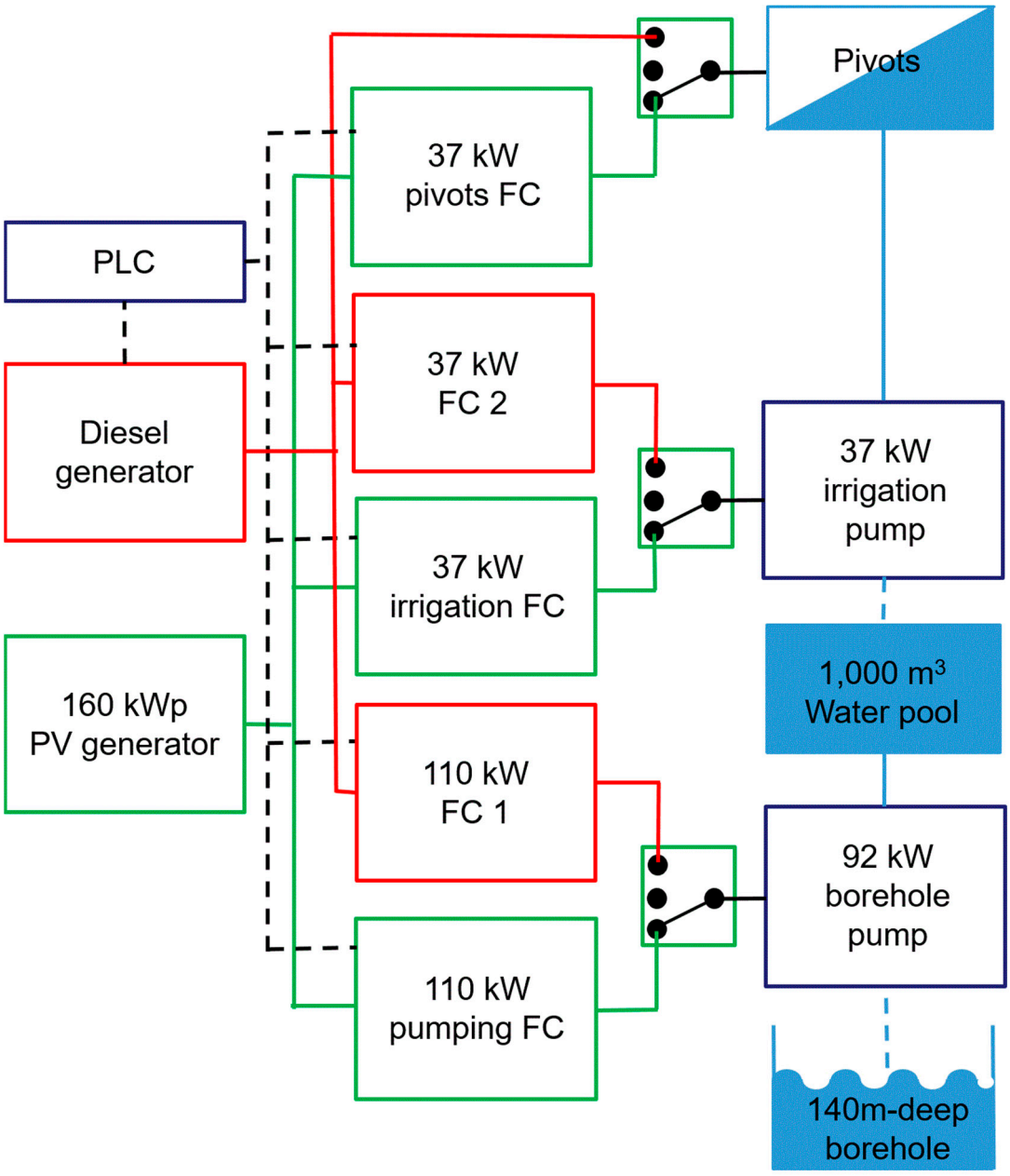

Figure 2. PVIS configuration: A PV generator, three FCs (all in green), and a PLC were added to the pre-existing configuration (diesel generator, two FCs in red, and two motor-pumps).

By definition, the PVIS is considered a stand-alone PV pumping system. However, since the pre-existing IS was kept, the whole PVIS could operate in three operation modes that the user could manually choose:

- PV mode: the entire IS is fed by the PV generator;
- PV/Diesel mode: pivots and the irrigation pump are fed by the PV generator while the borehole pump is fed by the diesel generator;
- Diesel mode: the diesel generator supplies the required power.

The IS was used in PV mode to pump the maximum volume of water during the day, using the diesel generator at times of low radiation or at night when the PV system could not cover all the water needs of the crop.

The PVIS included an external programmable logic controller (PLC) that, depending on the end-user irrigation needs, the selected operation mode, the estimated available PV

power, and the borehole and tank water levels, controlled the start and stop of the FCs. The PLC estimated the available PV power from irradiance measurements in the plane of the PV generator and cell temperature according to a maximum power point model [37] and gave the start order to the irrigation FC, to the pumping FC, or to both. Whenever the irrigator wanted to irrigate, the irrigation FC had priority over the pumping FC in case there was not enough PV power to make both pumps work. The PLC controlled the start and stop of the FCs based on hysteresis logic and a set of thresholds: one start threshold and one stop threshold to operate each FC. When the estimated available power was higher than the first start threshold (35 kW), the PLC sent a start signal to the irrigation FC, and the irrigation pump started operating. Another start signal was sent to the pumping FC when the estimated PV power was greater than a second start threshold (110 kW). If the estimated PV power fell below any stop threshold (51 kW for the second FC and 30 kW for the first one) during a 60 s time interval, a signal was sent to the corresponding FC to stop. Whenever the irrigation FC was on, the pivot FC was also on to power the motors that kept the pivots moving. Figure 3 schematically shows this hysteresis cycle.

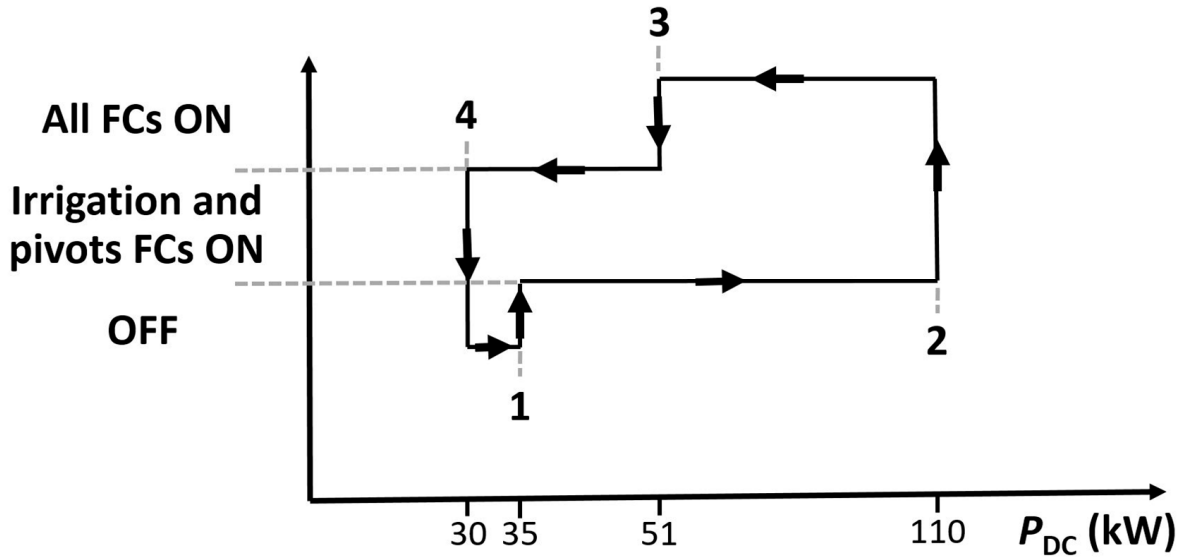

Figure 3. Available PV power thresholds with hysteresis for start and stop of the FCs, indicating when start and stop signals were sent (1—irrigation and pivots FCs start signal, 2—pumping FC start signal, 3—pumping FC stop signal, and 4—irrigation and pivots FCs stop signal).

Furthermore, in order to avoid start/stop cycles due to tank water levels, another hysteresis control based on four thresholds was used. When the tank water level was below a minimum threshold (L1) of 5% of the tank capacity, the tank was considered empty, and the irrigation FC was stopped. It was only started by the PLC when the tank water level reached a second threshold (L2), 10% of the tank capacity. Similarly, when the tank water level reached a maximum threshold (L4), 100% of the tank capacity, the pumping FC was stopped and only restarted when the water level dropped below L3 (90% of the tank capacity).

Besides the PLCs operating logic, all FCs had their own control programs. The pumping FC was controlled by a Maximum Power Point Tracking (MPPT) routine that maximized the efficiency of the PV production. The irrigation FC ran a pressure control routine to keep pressure at the irrigation network constant (there were three different pressure set points: 3, 4, and 5 bar, according to the pivot being used). In addition, the pivots FC was parameterized to work continuously at 50 Hz, simulating the grid. All FCs had passing cloud routines that allowed the PVIS to not be destabilized by fast irradiance fluctuations.

Figure 4 shows an aerial view of the PVIS, displaying the PV generator, the 1000 m^3 elevated water tank or water pool, the FC house, and the irrigation and borehole pumps.

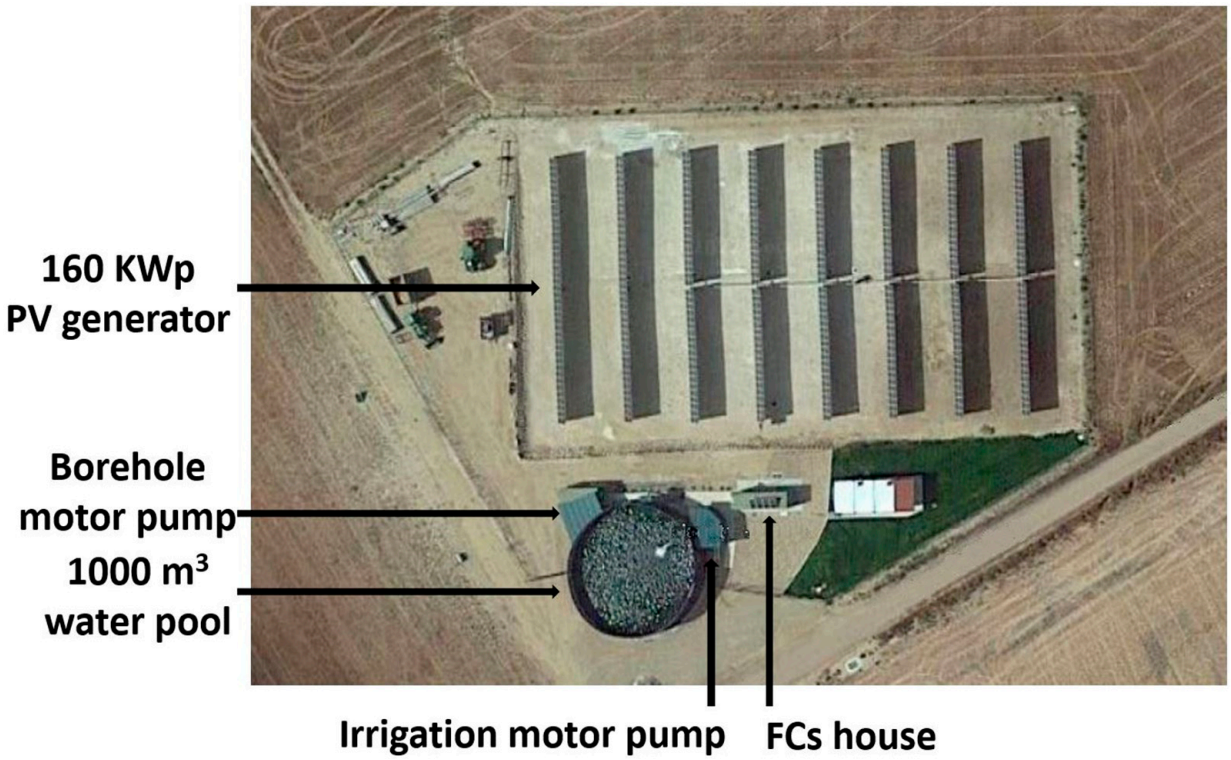

Figure 4. Aerial view of the PVIS in Alaejos.

The PVIS was monitored by means of one-minute records of the output frequency, direct current (DC) voltage (V_{DC}), DC current (I_{DC}), DC power (P_{DC}), alternating current (AC) voltage (V_{AC}), and AC current (I_{AC}) of the irrigation and pumping FCs, FC status, pressure and pressure set point for the irrigation network, irradiance (G), and module temperature (T_c).

2.2. Indicators Used to Assess the PVIS in Real Operating Conditions

The *PR* [37] has been traditionally used to analyze the performance of PV grid-connected plants. It is defined as

$$PR = E_{PV}/((P^*/G^*)\int Gdt), \quad (1)$$

where P^* is the peak power of the PV generator, G^* is the irradiance under standard test conditions (1000 W/m^2), G is the irradiance on the plane of the PV generator, and E_{PV} is the energy produced by the PV system. Due to their specificities, high-power PVIS include *PR* losses not only related to the quality of the PV system itself but also to the crop and its irrigation period (IP), the intrinsic characteristics of the PVIS design, the hydraulic infrastructure, and external circumstances that may affect the *PR*, like irrigator decisions. Considering these, the *PR* can be expressed as [34]

$$PR = \frac{E_{PV}}{P^*/G^*} \times \frac{1}{\int Gdt} \times \frac{\int_{IP} Gdt}{\int_{IP} Gdt} \times \frac{\int G_{useful}dt}{\int G_{useful}dt} \times \frac{\int G_{used}dt}{\int G_{used}dt}, \quad (2)$$

where

- IP is the irrigation period determined by the relationship between water needs, pumping capacity, and pumped water storage capacity in the case of pumping to a wa-

ter tank and by the water needs of the crop and climatic conditions in the case of direct pumping;

- G_{useful} (Figure 5c) is the irradiance required to deliver the power needed to elevate water to the water tank or to pump a given flow rate of water at the constant-pressure required by the pivots during the IP. It is determined by the relationship between the PV generator nominal power (P^*), the PV generator supporting structure, and the characteristics of the PVIS. When the available irradiance is below a minimum threshold, the pumps cannot start because there is not enough power. When the available irradiance is above G_{useful}, part of the irradiance is wasted because the PV generator cannot supply more power than that consumed by the pump working at its nominal power;
- G_{used} (Figure 5d) is the irradiance effectively used by the PVIS and depends on external circumstances like the availability of water or the irrigator's decisions about whether to irrigate or not.

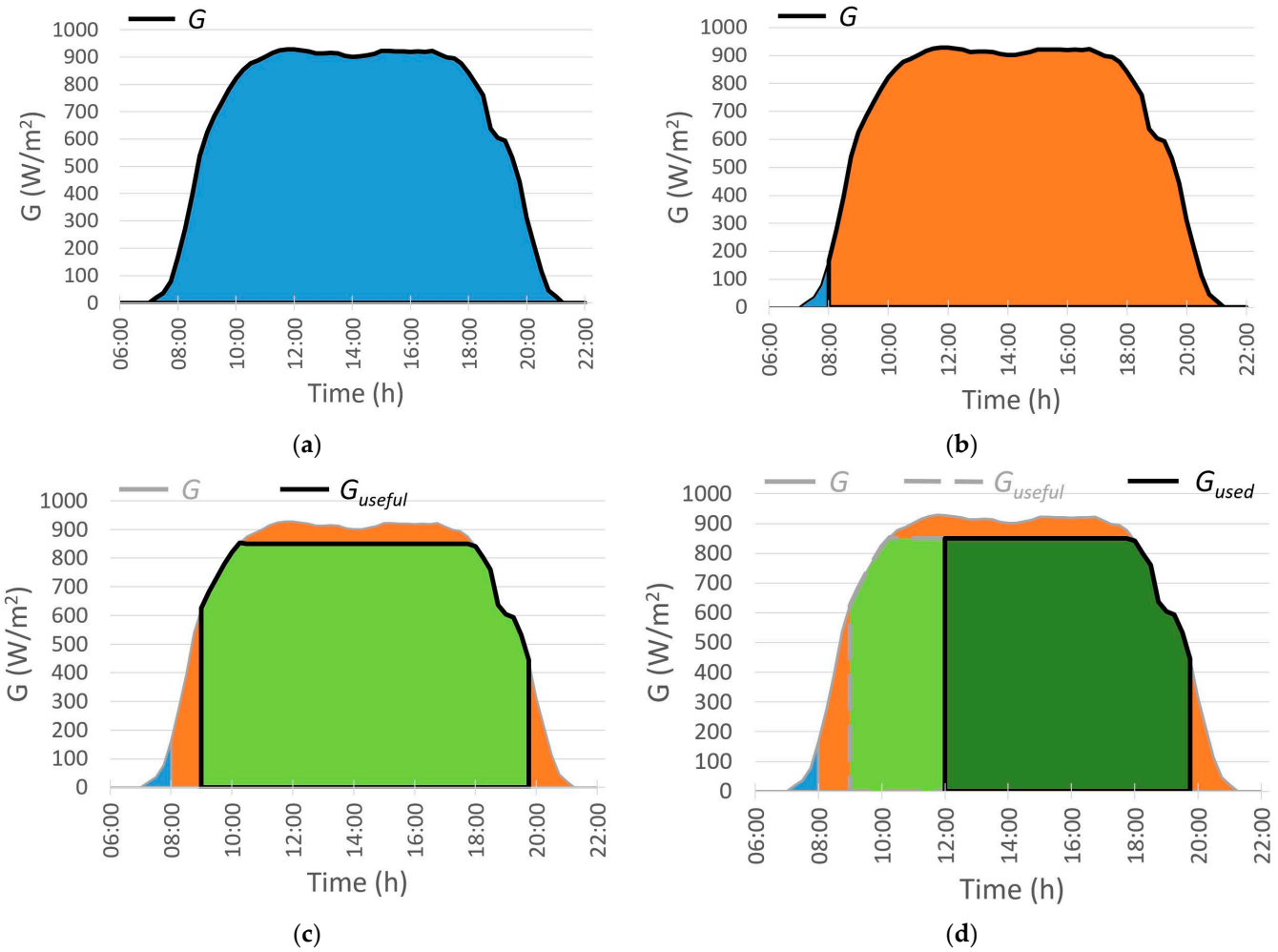

Figure 5. Graphical representation of: (**a**) $\int Gdt$ (blue area); (**b**) $\int_{IP} Gdt$ (orange area), where the irrigation period starts at 8:00 and ends after 23:00; (**c**) $\int G_{useful}dt$ (light green area), where the PVIS could be on from 9:00 to 19:45; and (**d**) $\int G_{used}dt$ (dark green area), where the irrigator decides to start the PVIS at 14:00.

Equation (2) can be rewritten as [34]

$$PR = PR_{PV} \times UR_{IP} \times UR_{PVIS} \times UR_{EF}, \quad (3)$$

where

$$PR_{\mathrm{PV}} = \frac{E_{\mathrm{PV}}}{P^*/G^*} \times \frac{1}{\int G_{\mathrm{used}} dt};\ UR_{\mathrm{IP}} = \frac{\int_{\mathrm{IP}} G dt}{\int G dt};\ UR_{\mathrm{PVIS}} = \frac{\int G_{\mathrm{useful}} dt}{\int_{\mathrm{IP}} G dt};\ UR_{\mathrm{EF}} = \frac{\int G_{\mathrm{used}} dt}{\int G_{\mathrm{useful}} dt} \quad (4)$$

PR_{PV} is the *PR* considering losses strictly related to the PV system itself; UR_{IP} is the utilization ratio considering losses related to the irrigation period; UR_{PVIS} is the utilization ratio considering losses related to the PVIS design (type of IS, the ratio PV peak power—PV power required for irrigation, the tracking geometry, and the accuracy of the PLC control algorithms); and UR_{EF} is the utilization ratio considering losses related to the irrigator's decisions.

In addition to the *PR*, Herraiz et al. [38] described the importance of two other indices to assess the correct functioning of PVIS: the number of abrupt stops and the passing cloud resistance ratio. The number of abrupt stops counts FC stops that occur suddenly and without control, as opposed to those initiated and controlled by the PLC or the FC itself that are performed gradually [38]. Under normal operating conditions, FCs stop in a controlled way. Abrupt FC stops are due to PVIS control instabilities caused by PV power quick intermittences or by a malfunction of the control. Distinguishing abrupt stops from controlled stops is important to correctly classify the losses associated with each stop. An abrupt stop is considered a PVIS malfunction, and the resulting losses are accounted for in the PR_{PV}. Conversely, losses associated with controlled stops are accounted for in the UR_{PVIS} as they are related to the PVIS design. In order to distinguish between abrupt and controlled stops, it is necessary either that the monitoring system records information about the type of stop or that the PVIS is monitored by means of one-second records.

The passing cloud resistance ratio (σ_{cloud}) is defined as $\sigma_{cloud} = \#\ resisted\ clouds / \#\ clouds$, where "# resisted clouds" is the number of passing clouds (big PV power fluctuations in short periods) that do not lead to FC abrupt stops and "# clouds" is the total number of passing clouds in a specific period of time [38]. In order to calculate this index, a monitoring system with one-second records is required.

2.3. Data Filtering

The effects of data availability, filtering, and quality are becoming increasingly important in the PV sector, both in the literature and in industry [39–41]. The number of PV systems and their size are undergoing exponential growth in all areas, causing management and analysis procedures to become more complex. Data quality affects performance calculations. The quality of operating condition measurements is particularly relevant since the linearity of these variables with respect to the power shown by the models constitutes a powerful indicator of anomalies. To ensure adequate data quality, operating conditions and production data were filtered using three different types of filters, as stated in the IEC standard IEC-61724-2 [42]:

- Range filter. This filter discards all values outside an established range for each analyzed variable. Minimum and maximum thresholds are defined, and any data that do not meet the requirements are removed. The threshold values are defined according to the season of the year. Therefore, there are four filter ranges for Spring, Summer, Autumn, and Winter.
- Dead Value Filter. This type of filter discards frozen values, assuming that variables that maintain their value over time have abnormal behavior. Two parameters are required to implement it: the necessary minimum variation between analyzed periods to consider that a value is not frozen, and the minimum threshold from which the filter is applied (for example, the dead value filter may be applied to the measured power only when it is greater than zero).
- Abrupt Change Filter. Analyzes the variation of the values of each variable between two-time intervals, discarding all values whose variation exceeds a certain threshold. This filter removes values that have changed faster than what is considered normal.

The previous filters were used to filter outliers from normalized data and try to eliminate measurement errors and noise, especially in operating condition variables (such as irradiance and temperature) and also in other critical production variables such as current, voltage, and power. In addition to these filters, coherence filtering was applied to remove inconsistent values, such as night-time irradiance values greater than zero.

Another major problem in the monitoring of stand-alone PVIS is the loss or absence of data. The causes can be multiple, including measurement problems, communication failures, problems in the data acquisition system, or outputs of the applied filters. This lack of data affects performance evaluation and monitoring fault detection, leading to a reduction in the PV system's lifetime. As in data filtering, data losses are especially relevant when they affect operating conditions. Loss of meteorological data causes underestimation of in-plane irradiation (and overestimation of *PR*), while gaps in electrical data could be filled and still estimate with precision the energy yield. This study solved the problem of missing data by representing it as null values to clearly differentiate missing values from other types of problems when analyzing the data and by excluding the affected periods from processing.

2.4. Data Processing

After filtering the data were processed to obtain the performance indices. The first step of this process aimed to identify FC stops and whether these stops were controlled or abrupt. One FC stopped because its status changed from "running" to "stopped". Moreover, a specific status indicated that a stop was abrupt, thus distinguishing controlled stops from abrupt stops. As stated above, distinguishing abrupt from controlled stops is important to correctly classify the losses associated with each stop. An abrupt stop is considered a PVIS malfunction, and the resulting losses are accounted for in the PR_{PV}. Conversely, losses associated with controlled stops are accounted for in the UR_{PVIS}, as they are related to the PVIS design, or in the UR_{EF}, when they are a consequence of the irrigator's decisions. Stops for PVIS maintenance receive special treatment. Preventive maintenance actions have to take place outside the IP or at night in order to not affect the *PR*. Preventive maintenance actions during the IP and during the daytime were accounted for in the UR_{EF} as a decision of the irrigator. Finally, corrective maintenance actions (a stop for the repair of malfunctioning equipment) are accounted for in the PR_{PV}. However, several situations have been detected that hinder this processing due to the limitations of the monitoring of the PVIS under study. On the one hand, there are situations in which the FC status field indicates that the FC is stopped, but the rest of the variables (*frequency*, I_{DC}, V_{DC}...) show the opposite. To compensate for this, a double validation by status and I_{DC} was performed for each FC. On the other hand, situations involving the abrupt stop of an FC are not always recorded. The monitoring system collected data every minute and stored the value of each variable at the precise moment it was recorded. It is possible that an abrupt stop occurred, but the FC status variable was not picked up until several seconds later. In that interval, the FC status could have changed from abrupt to controlled, masking the type of FC stop. It is also possible that a FC stops abruptly during the start-up process and the start-up status is not registered.

PVIS with one-second monitoring allowed us to identify, in addition to abrupt and controlled stops, passing clouds over the PV generator and whether they are resisted (do not alter the operation of the PVIS) or not (cause an abrupt stop of the FCs). Since the monitoring system of the PVIS under study only collected data every minute, it was not possible to obtain these indices in the present work.

The second processing step consisted of obtaining the ideal PVIS behavior map from the available operating conditions data (in-plane irradiance and cell temperature). The behavior map shows what time each FC should be started and how long it should be on, as well as the number of FCs that should be on simultaneously at each moment. This ideal map can be compared with the real map of the PVIS obtained from the production data. The actual map differs from the ideal for several reasons: it is affected by controlled stops

not predictable from operating conditions and by abrupt stops of the FCs; it is altered by the existing water level in the intermediate tank (pumping from the borehole is prevented when the tank is full, and irrigation is not possible when it is empty); and it is highly dependent on the behavior of the end user.

Significant events were identified and classified:

- The absence of data on operating conditions;
- Time that is not part of the IP;
- Events related to the irrigator's use of the PVIS (such as the use of the PV/Diesel or Diesel modes or manual stops caused by the irrigator);
- Events directly associated with the IS (such as a lack of water in the tank when the irrigator wants to irrigate or a full tank).

The event information (type and time at which they begin and end) was used, together with the stop information and the behavior maps (the ideal and actual ones), to calculate the utilization ratios and the *PR*.

When processing the data, a PV generator power equal to the measured actual power (150.3 kWp) was considered. Since the monitoring system does not record data from the pivot FC, the FC efficiency and the consumption of the motors that move the pivots were also measured (92.0% and 4.5 kW, respectively), considering an average P_{DC} for the pivot FC of 4.5 kW whenever the irrigation FC was on.

3. Results

This study analyzed the data collected and the behavior of the PVIS between May 2019 and August 2022. During this time interval, the IP of each season was the same, starting on March 15 of each year and ending on October 15. However, since 2019, data were only available from the end of April, and in order to analyze and compare full-year data, each year under study was determined to start in May and end in April of the following year. Thus, the data presented below show the results for three full years of PVIS operation: from May 2019 to April 2020 (the first year), from May 2020 to April 2021 (the second year), and from May 2021 to April 2022 (the third year).

3.1. Number of Stops

FC stops are due to operating conditions (when irradiance drops below the minimum necessary threshold, the FC stops), IS limitations (if the intermediate tank is empty, the irrigation FC stops, and if it is full, the pumping FC stops), direct irrigator actions (the irrigator stops a FC to change the irrigation program, because he does not want to continue irrigating, or for any other reason), and control instabilities (caused, for example, by abrupt variations in available power due to passing clouds).

Tables 1–3 show the total number of abrupt and controlled stops per month and per day for each year, considering only days for which information is available and in which the FCs have been working. In all tables, FC 1 refers to the irrigation FC and FC 2 refers to the pumping FC. Pivot FC stops are not shown in the tables because the pivot FC was not monitored. In any case, since the pivot FC is always on during irrigation, it is started and stopped together with the irrigation FC, both having the same number of stops.

The number of days for which the data were available and the FCs were active in each month reflected that the period from mid-October to mid-March did not belong to the IP. However, during the third year of study, an activity increase can be seen in that period. Single days were used to fill the intermediate tank or for occasional irrigation. The low number of operating days in some months of the IP (e.g., August and September 2019) is also striking. This was due to a failure in the monitoring system, which was blocked and stopped storing information.

Tables 1–3 show that the total number of stops per day and per FC remained stable throughout the three years of PVIS operation. During the first year, the irrigation FC stopped an average of 3.62 times per day (3.29 + 0.33), 3.49 per day (3.26 + 0.23) during the second year, and 3.4 times in the third year (3.15 + 0.25). This represents a reduction in

the total number of stops per day of 6.1% from the first year to the third. Regarding the pumping FC, the first year it stopped an average of 5.92 times per day (5.45 + 0.47), the second year 6.33 (5.9 + 0.43), and the third year 6.25 (6 + 0.25). This represents an increase in the number of stops per day of 5.6% between the first year and the last. The number of stops for the pumping FC was higher than that for the irrigation FC. This is because the PLC gives priority to the irrigation FC over the pumping FC whenever the irrigator wants to irrigate, so when irradiance decreases, the first FC to stop is the pumping FC. The percentage of abrupt stops in the pumping FC (7.9% the first year, 6.8% the second, and 4.0% the third) decreased over time. The percentage of abrupt stops in the irrigation FC (9.0%, 6.7%, and 7.5%, respectively) was of the same order of magnitude as in the pumping FC, with no clear trend in its evolution over time.

Table 1. Number of stops of each FC during the first year.

Year	Month	Days FC 1/FC 2	Controlled Stops FC 1	Abrupt Stops FC 1	Controlled Stops FC 2	Abrupt Stops FC 2
2019	05	31	132	13	192	30
	06	30	114	8	194	16
	07	31	106	5	123	29
	08	16/15	45	4	89	3
	09	20	54	3	111	1
	10	17/18	47	12	95	1
	11	0	0	0	0	0
	12	0	0	0	0	0
2020	01	0	0	0	0	0
	02	0	0	0	0	0
	03	13/16	30	2	74	0
	04	17/11	48	10	56	0
Total		175/172	576 (91.0%)	57 (9.0%)	938 (92.1%)	80 (7.9%)
Total per day		**-**	**3.29**	**0.33**	**5.45**	**0.47**

Table 2. Number of stops of each FC during the second year.

Year	Month	Days FC 1/FC 2	Controlled Stops FC 1	Abrupt Stops FC 1	Controlled Stops FC 2	Abrupt Stops FC 2
2020	05	27	90	1	154	12
	06	30	129	6	289	28
	07	29	71	9	117	16
	08	31	93	18	171	17
	09	22/19	40	11	77	9
	10	16/18	65	1	124	0
	11	0	0	0	0	0
	12	0	0	0	0	0
2021	01	0/6	0	0	4	4
	02	0	0	0	0	0
	03	16/17	56	0	61	2
	04	30/29	111	1	218	1
Total		201/206	655 (93.3%)	47 (6.7%)	1215 (93.2%)	89 (6.8%)
Total per day		**-**	**3.26**	**0.23**	**5.9**	**0.43**

Table 3. Number of stops of each FC during the third year.

Year	Month	Days FC 1/FC 2	Controlled Stops FC 1	Abrupt Stops FC 1	Controlled Stops FC 2	Abrupt Stops FC 2
2021	05	31	105	1	255	6
	06	28/27	98	5	172	14
	07	31	105	6	133	11
	08	31	76	14	110	12
	09	25	88	11	205	3
	10	24/28	95	8	161	0
	11	4/11	6	0	28	11
	12	0/4	0	0	12	0
2022	01	0	0	0	0	0
	02	18	53	6	103	1
	03	12/14	29	3	103	0
	04	24/27	63	4	199	4
Total		228/248	719 (92.5%)	58 (7.5%)	1487 (96.0%)	62 (4.0%)
Total per day		**-**	**3.15**	**0.25**	**6**	**0.25**

3.2. Performance Ratio

Tables 4–6 show the experimental monthly values of the performance indices.

Table 4. Experimental monthly values of the performance indices (%) for the first year.

Year	Month	PR_{PV}	UR_{IP}	UR_{PVIS}	UR_{EF}	PR
2019	05	80.7	100	83.7	92.7	62.6
	06	80.6	100	80.8	94.0	61.2
	07	77.9	100	87.9	92.8	63.6
	08	79.7	100	80.3	95.0	60.8
	09	86.4	100	82.2	93.1	66.1
	10	86.3	75.9	81.3	97.1	51.7
	11	-	0	-	-	0.0
	12	-	0	-	-	0.0
2020	01	-	0	-	-	0.0
	02	-	0	-	-	0.0
	03	84.1	100	60.6	92.0	46.8
	04	78.1	100	27.0	62.6	13.2
	Total	**80.9**	**87.9**	**75.9**	**92.3**	**49.8**

Table 5. Experimental monthly values of the performance indices (%) for the second year.

Year	Month	PR_{PV}	UR_{IP}	UR_{PVIS}	UR_{EF}	PR
2020	05	79.9	100	76.0	92.5	56.2
	06	78.8	100	82.5	97.7	63.5
	07	75.4	100	79.2	95.2	56.8
	08	77.1	100	84.8	95.9	62.7
	09	79.2	100	61.8	84.1	41.2
	10	82.5	80.9	76.5	93.1	47.5
	11	-	0	-	-	0.0
	12	-	0	-	-	0.0
2021	01	89.2	9.2	92.7	100	7.6
	02	-	0	-	-	0.0
	03	80.0	66.1	80.0	87.6	37.1
	04	83.5	100	80.1	96.5	64.5
	Total	**79.0**	**84.7**	**78.0**	**93.8**	**49.0**

Table 6. Experimental monthly values of the performance indices (%) for the third year.

Year	Month	PR_{PV}	UR_{IP}	UR_{PVIS}	UR_{EF}	PR
2021	05	81.4	100	81.2	95.7	63.3
	06	80.2	100	81.8	92.2	60.5
	07	80.4	100	88.6	98.1	69.9
	08	79.7	100	92.8	97.5	72.1
	09	82.2	100	64.8	95.3	50.8
	10	82.8	96.8	78.6	98.2	61.9
	11	84.2	17.7	92.9	96.1	13.3
	12	72.6	1.3	72.8	100	0.7
2022	01	94.1	0.7	51.4	100	0.3
	02	83.3	63.3	89.2	96.9	45.6
	03	86.2	82.2	56.8	60.6	24.4
	04	67.6	100	80.3	95.6	51.9
	Total	**79.4**	**87.2**	**81.2**	**94.7**	**53.2**

The PR_{PV} values (80.9% for the whole first year) were slightly below the PR values expected for grid-connected PV systems.

UR_{IP} was 100% from May to September and in April, lower than 100% in October, and 0% from November to January, resulting in a yearly value of 87.9%. It is striking that the March 2020 UR_{IP} was 100% considering that half of that month did not belong to the *IP*. It would have been reasonable to expect a lower value, close to 50%, in line with the values of days of operation of the FCs indicated in Table 5 (13 days for the irrigation FC and 16 for the pumping FC). The 100% value was due to the failure of the monitoring system from February 12 to March 16 and the exclusion of this interval from the study; we only analyzed the days between March 16 and 31, all of which were part of the IP.

The UR_{PVIS} first year value was 75.9%. Compared to those reported by [38] for PVIS pumping to a water pool (75.6% and 85.2%), the obtained value was similar to the first and lower than the second. It is reasonable to expect a lower UR_{PVIS} for a constant flow and constant-pressure PVIS than for a PVIS pumping to a water pool, in which the flow of pumped water can be adjusted to the available PV power. In constant-pressure and constant flow PVIS, power consumption is also constant, and the FC does not start until the irradiance reaches a threshold that allows the required PV power to be generated. The PV power that could be generated at all times of the day when the irradiance is below this threshold is lost. Similarly, the power that could be generated when the irradiance is above the threshold is lost because the PVIS cannot consume more power than necessary to achieve the pressure required by the pivots. In addition, the small size of the intermediate water tank also decreased UR_{PVIS} as the irrigation FC stopped when the tank was empty, and the borehole FC stopped when the tank was full.

The UR_{EF} value (92.3%) was smaller than expected (close to 100%). The possibility of using the diesel or PV/diesel modes and the water needs of the crop led the irrigator to use the diesel mode at night, at times of low irradiance, and when the intermediate tank was empty. The delay in switching to PV mode when the irradiance allowed it or when there was enough water in the tank to keep on irrigating caused the UR_{EF} to worsen. This effect was increased by the long stops of the PVIS when the irrigator changed the irrigation program.

The PR value was close to 50% (49.8%) due to the combined effect of all the previous indices, but especially UR_{IP} (highly dependent on the crop), UR_{PVIS}, and UR_{EF}.

The values obtained for the second and third years did not differ radically from those of the first year. The PR value for the second year (49.0%) was smaller than the 49.8% of the first year, mainly because of the decrease in the UR_{IP} due to proper accounting of the month of March. If this month had been correctly accounted for in the first year, the final PR value would have been even lower than the 49.0% of the second year (assuming for the first year the same total UR_{IP} value as the second year, 84.7%, the total PR would have been

48.0%). On the other hand, the *PR* improved for the third year (53.2%). Although the PR_{PV}, which measures the quality of the PV system itself, decreased with respect to the first year, an improvement was observed for the rest of the indices. This improvement was caused by a longer IP (an increased usage in February), an improved use of the intermediate water tank, and, in general, a better use of the PVIS by the irrigator. The evolution of the indices over the three years can be seen in Table 7.

Table 7. Experimental annual values of the performance indices (%).

Period	PR_{PV}	UR_{IP}	UR_{PVIS}	UR_{EF}	*PR*
2019-05 to 2020-04	80.9	87.9	75.9	92.3	49.8
2020-05 to 2021-04	79.0	84.7	78.0	93.8	49.0
2021-05 to 2022-04	79.4	87.2	81.2	94.7	53.2

4. Discussion

Stand-alone high-power PV irrigation systems with no batteries are relatively new, and there are not enough data available in the literature on their expected experimental performance values. It is useful to establish the thresholds required in the quality control procedures associated with contractual frameworks for the sale and installation of this type of PVIS. This section discusses the experimental results of the different performance indices found in this analysis.

4.1. Expected PR Values for High-Power PVIS Combining Pumping to an Intermediate Tank and Direct Pumping to an IS Based on Pivots

This study began with the intuition that the *PR* of constant-pressure PVIS should be lower than that for PVIS pumping to a water pool. PVIS pumping to a water pool work at variable frequency. They adapt the FC output frequency to the available PV power, varying the pumped flow at each moment. When the available PV power is low, the FC output frequency is low. The operating frequency and the pumped flow rate increase as the available PV power increases up to the maximum allowed by the pump, thus working in a range of frequencies. In contrast, direct pumping PVIS operates at a constant flow and pressure. To provide that flow and pressure, the motor pump has to work at a certain frequency, consuming a specific amount of power. The FC does not start until the irradiance reaches a threshold that allows the required PV power to be generated. The power that could be generated at all times of the day when the irradiance is below this threshold is lost. Similarly, some of the PV power that could be generated when the irradiance is above the threshold is lost because the PVIS cannot consume more power than necessary to achieve the pressure required by the pivots. The system works at a single frequency instead of several frequencies and consumes a certain power instead of a range of powers, thus making less use of the available PV power. This is a feature associated with the PVIS design. Therefore, when factorizing the *PR*, a decrease in the UR_{PVIS} (the utilization ratio that takes into account losses of this type) should be observed.

The PVIS under study was not strictly a constant-pressure IS. It combined three FCs. The irrigation FC was typical of a constant-pressure IS, the pumping FC was typical of a PVIS pumping to a water pool, and the pivots FC had constant consumption whenever irrigation was taking place. This variety of FCs and their different power ratings mitigated the reduction in UR_{PVIS}, but it should still be observed.

4.1.1. UR_{PVIS} Values

The results showed annual UR_{PVIS} values between 75.9% and 81.2%, which represents a decrease between 4.7% and 10.9% with respect to the values reported by [38] for Villena PVIS pumping to a water pool (Aldeanueva's value was not used as a reference because it was affected by the oversizing of the PV generator, which caused a reduction in the UR_{PVIS}). This decrease was in line with what was expected prior to the start of the study.

The data also showed an improvement in UR_{PVIS} over time (from 75.9% to 78.0% and 81.2%) that can be explained by the improvement in the use of the intermediate tank. The irrigator used the diesel mode at night and at times of low irradiance and the PV/Diesel mode during the day when the tank was empty, reducing the full/empty tank time during the day. The other factors that affected UR_{PVIS} did not change: the power of the PV generator, the size of the intermediate tank, the ratio of PV peak power to PV power required for irrigation, the irrigated land, the irrigation programs, and the pressures required by the pivots. The number of controlled stops per day due to low levels of irradiance (and the time the PVIS remained stopped for safety after each stop) does not explain the improvement in UR_{PVIS} either, as it did not change over the three years (8.7 controlled stops per day the first year, 9.16 the second, and 9.15 the third).

The relationship between the improvement of UR_{PVIS} and the reduction of full/empty tank times can be seen in Table 8, which shows that when the number of minutes per day that the tank is full or empty increases, UR_{PVIS} decreases. The table shows no relationship between the evolution of UR_{PVIS} and the number of controlled stops. The months of July and August were chosen as the months with the highest UR_{PVIS}. The high temperatures of these months resulted in lower production and, therefore, lower limitations due to excess power in the constant-pressure PVIS.

Table 8. Monthly UR_{PVIS}, time the intermediate tank remains empty or full (in minutes per day, considering only the interval between 7:00 and 19:00 UTC), and the number of controlled stops per day for the months of July and August over the three years.

$\boldsymbol{UR_{PVIS}}$ (%)	92.8	88.6	87.9	84.8	80.3	79.2
Full/empty-tank time (minutes per day)	21	25	30	71	101	134
Controlled stops (per day)	6.0	10.3	7.4	8.5	8.9	6.5
Month	2021-08	2021-07	2018-07	2020-08	2019-08	2020-07

Even though the times in which the tank was full or empty were counted together, it is important to note that the impact of a full tank is not the same as that of an empty tank. Moreover, the impact also depends on the corrective action taken by the irrigator: using the diesel mode, the PV/diesel mode, or leaving the PV on.

The above data suggested that, once the learning curve of the use of the PVIS has been traversed, during which the UR_{PVIS} improved due to the use of the intermediate tank, this index will not improve any further. Therefore, the expected UR_{PVIS} losses in a constant-pressure PVIS, such as the one studied, with respect to a PVIS pumping to a water pool can be quantified at around 5%, and it is reasonable to expect UR_{PVIS} values of 80% for this type of system.

4.1.2. PR_{PV} Values

The PR_{PV} annual values (80.9%, 79.0%, and 79.4%) were slightly lower than the PR values expected for grid-connected PV systems. Temperature losses do not explain the difference. PR_{PV} values under standard test conditions (89.3%, 87.1%, and 87.1%, respectively) were still low compared to those expected for grid-connected PV systems (and lower than the 95.7% reported by [38] for the Aldeanueva PVIS). Abrupt stops introduced by control instabilities associated with the IS do not explain the existing difference either, especially if we take into account that the number of abrupt stops detected may be lower than the real number. The data showed that it is reasonable to expect PR_{PV} values over 80.0%.

4.1.3. UR_{IP} Values

UR_{IP} is very dependent on the crop and climate conditions where the PVIS is located. In a direct pumping PVIS, these two factors determine the irrigation period. When pumping to a water pool or an intermediate tank, the IP can be extended. The additional extension depends on the capacity of the tank. In the PVIS under study, the IP started on March

15 and ended on October 15, and in the third year, it was extended a few days more. The 1000 m^3 intermediate tank did not allow the IP to be extended any further. Under these conditions, it is reasonable to assume that the UR_{IP} will remain around 85%.

4.1.4. UR_{EF} Values

UR_{EF} values improved every year (from 92.3% to 93.8% and 94.7%), which indicates a better use of the PVIS by the irrigator. The time the system was down as a result of controlled stops caused by the irrigator was also reduced. As an example, the number of minutes it was down per day in July and August (considering only the interval between 7:00 and 19:00 UTC) was reduced by 21.6% from the first to the second year and by 81.4% from the first to the third year, and the time it was working in diesel or PV/diesel mode was reduced by 45.7% and 29.8%, respectively. A proper use of the PVIS by the irrigator (not using the diesel or PV/diesel modes when there is enough irradiation to use the PV mode, avoiding manual shutdowns, PV irrigation schedule centered at midday, planning of maintenance tasks on cloudy days or at night, management of water consumption) would lead to values very close to 100%, as seen in our results.

PR_{PV}, UR_{IP}, UR_{PVIS}, and UR_{EF} determine the PR values. The PR values obtained experimentally were between 49.0 and 53.2%. The expected values for each index (PR_{PV} >= 80%, UR_{IP} >= 85%, UR_{PVIS} >= 80%, and UR_{EF} = 100%) suggest that it is reasonable to expect PR values around 55% in high-power constant-pressure PVIS.

4.2. Number of Abrupt Stops

Since abrupt stops can cause water hammers and AC over-voltages that seriously threaten the reliability of both the hydraulic and electric components of the PVIS, a reduced number of abrupt stops reduces the risks.

The current study was not decisive in relation to the maximum number of abrupt stops that can be expected from a PVIS with these characteristics or the relationship between the number of abrupt and controlled stops that is advisable. The difficulties encountered in identifying the type of stop prevented this. Stops listed in the tables as abrupt for each inverter were indeed abrupt, but there is no certainty that stops listed as controlled were actually all controlled. A detailed analysis of the data suggested that the percentage of abrupt stops could be higher than that shown in the tables. Multiple FC stops occur in typical passing cloud situations (irradiance drops abruptly for a short interval and then recovers). In these situations, the FC should stop in a controlled way if the irradiance remains for more than one minute below a given threshold, and it should remain on in any other case. Due to the characteristics of the monitoring system, which records data only every minute, it was not possible to know the exact duration of the irradiance drop or whether the drop was sustained for a minute or not. The high number of FC stops in passing cloud circumstances lead us to suspect that not all of them were due to irradiance drops lasting more than one minute. Therefore, some of the FC stops may have been due to control instabilities and have been abrupt, although the monitoring system did not always record them. To confirm the suspicion that the number of abrupt stops were higher than that recorded, a monitoring system is needed that records data every second or records the abrupt stop status accurately. If a high number of abrupt stops was confirmed, the PVIS would have to be tuned to improve its performance.

5. Conclusions

Stand-alone battery-free, high-power PV irrigation systems are emerging as an alternative to high-power diesel-based or grid-connected irrigation systems. As a recent innovation, there is not enough experimental data available on their performance. A few performance data are available for PVIS pumping to a water pool, but no data are available for constant-pressure PVIS, although their design characteristics suggest a reduction in PR. This paper is a contribution to the experimental performance data of a constant-pressure center-pivot PVIS and, thus, to the expected values for other similar systems.

To assess the PVIS performance, the traditional *PR* was factorized into four factors: PR_{PV}, UR_{IP}, UR_{PVIS}, and UR_{EF}. PR_{PV} evaluates the performance quality of the PV system itself. UR_{IP}, UR_{PVIS}, and UR_{EF} measure the effect of the crop irrigation period, losses due to the IS design, and losses due to user behavior, respectively. In order to calculate these indexes, the FC stops were identified and classified as controlled, abrupt, automatic, or caused by the irrigator. Secondly, the ideal behavior map of the PVIS was obtained from the available data on operating conditions (irradiance and temperature) and the real map of the plant, which was obtained from the production data. Next, significant events were identified and classified (absence of operating conditions data, duration of the irrigation period, use of the PV/diesel or diesel modes, when the irrigator manually stops the PVIS, and other events such as a full or empty tank). Finally, event and stop information and PVIS operation maps (the ideal and actual ones) were processed to calculate the utilization ratios and the *PR*.

The results showed annual UR_{PVIS} values between 75.9% and 81.2%, annual PR_{PV} values between 79.0% and 80.9%, annual UR_{IP} values between 84.7% and 87.9%, annual UR_{EF} values between 92.3% and 94.7%, and *PR* values between 49.0% and 53.2%.

The two indices that had the greatest impact on *PR* were UR_{PVIS} and PR_{PV}. The former is intrinsic to the PVIS design, and the latter is conditioned by the quality of the PV system itself. The most important factor influencing the UR_{PVIS} is the fact that the PVIS works at constant-pressure. Working at constant-pressure means that the FC does not start until the available PV power reaches the power needed to operate the pump at the pressure required by the pivots, and that the additional PV power that the generator could supply if conditions improve is wasted. The impact of this feature on UR_{PVIS} was a 5% decrease over PVIS pumping to a water pool. The second element that most affects UR_{PVIS} is related to the size of the tank and the irrigator's management of it. This factor can be improved with proper training of the irrigator.

Relevant conclusions can be drawn from the results regarding the performance that can be expected: The expected *PR* in a good-quality constant-pressure PVIS is around 55%. The expected values for the different factors are $PR_{PV} >= 80\%$, similar to those expected in grid-connected PV systems; $UR_{IP} >= 85\%$; $UR_{PVIS} >= 80\%$; and $UR_{EF} \approx 100\%$ if the end user makes appropriate use of the PVIS. It is necessary to confirm these expected values with experimental measurements in other high-power constant-pressure PVIS, but these preliminary results may help to establish the technical thresholds to ensure the technical quality of these systems in the context of quality control procedures associated with contracts for the sale and installation of this type of system.

Author Contributions: Conceptualization, J.I.H. and L.N.; data curation, J.I.H. and M.C.-C.; formal analysis, J.I.H.; funding acquisition, L.N.; investigation, J.I.H., R.H.A. and L.N.; methodology, R.H.A. and L.N.; project administration, L.N.; resources, J.I.H., M.C.-C. and L.N.; software, J.I.H. and M.C.-C.; supervision, L.N.; validation, J.I.H.; visualization, J.I.H.; writing—original draft, J.I.H.; writing—review and editing, J.I.H., R.H.A., M.C.-C. and L.N. All authors have read and agreed to the published version of the manuscript.

Funding: This research was made possible thanks to funding from the European Union's Horizon 2020 research and innovation program for the SOLAQUA project under grant agreement Nº 952879 and thanks to the European Union's Horizon 2020 research and innovation program to SERENDI-PV project under grant agreement Nº 953016.

Data Availability Statement: Not applicable.

Conflicts of Interest: The authors declare no conflict of interest. The funders had no role in the design of the study, in the collection, analysis, or interpretation of data, in the writing of the manuscript, or in the decision to publish the results.

References

1. Palz, W. The French Connection: The rise of the PV water pump. *Refocus* **2001**, *2*, 46–47. [CrossRef]
2. Barlow, R.; McNelis, B.; Derrick, A. Solar pumping: An introduction and update on the technology, performance, costs, and economics. *World Bank Tech. Pap.* **1993**, *168*, 12.
3. Abella, M.A.; Lorenzo, E.; Chenlo, F. PV water pumping systems based on standard frequency converters. *Prog. Photovolt. Res. Appl.* **2003**, *11*, 179–191. [CrossRef]
4. Sontake, V.C.; Kalamkar, V.R. Solar photovoltaic water pumping system—A comprehensive review. *Renew. Sustain. Energy Rev.* **2016**, *59*, 1038–1067. [CrossRef]
5. Chabour, H.E.; Pardo, M.A.; Riquelme, A. Economic assessment of converting a pressurised water distribution network into an off-grid system supplied with solar photovoltaic energy. *Clean Technol. Environ. Policy* **2022**, *24*, 1823–1835. [CrossRef]
6. Zegait, R.; Bentraia, M.R.; Bensaha, H.; Azlaoui, M. Comparative Study of a Pumping System Using Conventional and Photovoltaic Power in the Algerian Sahara (Application to Pastoral Wells). *Int. J. Eng. Res. Afr.* **2022**, *60*, 63–74. [CrossRef]
7. Skibko, Z.; Romaniuk, W.; Borusiewicz, A.; Derehajło, S. Electricity supply to irrigation systems for crops away from urban areas. *J. Water Land Dev.* **2022**, *53*, 73–79. [CrossRef]
8. Saady, I.; Karim, M.; Bossoufi, B.; Motahhir, S.; Majout, B.; Salime, H.; Laabidine, N.Z. Study of a Photovoltaic Pumping System Application for Irrigation the Palm in Beni Mellal City. In *Lecture Notes in Networks and Systems*; Springer: Cham, Switzerland, 2022; Volume 454. [CrossRef]
9. Zavala, V.; López-Luque, R.; Reca, J.; Martínez, J.; Lao, M. Optimal management of a multisector standalone direct pumping photovoltaic irrigation system. *Appl. Energy* **2019**, *260*, 114261. [CrossRef]
10. Miran, S.; Tamoor, M.; Kiren, T.; Raza, F.; Hussain, M.I.; Kim, J.-T. Optimization of Standalone Photovoltaic Drip Irrigation System: A Simulation Study. *Sustainability* **2022**, *14*, 8515. [CrossRef]
11. Kumar, L.A.; Lakshmiprasad, C.N.; Ramaraj, G.; Sivasurya, G. Design, simulation of different configurations and life-cycle cost analysis of solar photovoltaic–water-pumping system for agriculture applications: Use cases and implementation issues. *Clean Energy* **2022**, *6*, 335–352. [CrossRef]
12. Ledesma, J.R.; Almeida, R.H.; Narvarte, L. Modeling and Simulation of Multipumping Photovoltaic Irrigation Systems. *Sustainability* **2022**, *14*, 9318. [CrossRef]
13. Gasque, M.; González-Altozano, P.; Gutiérrez-Colomer, R.P.; García-Marí, E. Optimisation of the distribution of power from a photovoltaic generator between two pumps working in parallel. *Sol. Energy* **2020**, *198*, 324–334. [CrossRef]
14. Farrar, L.W.; Bahaj, A.S.; James, P.; Anwar, A.; Amdar, N. Floating solar PV to reduce water evaporation in water stressed regions and powering water pumping: Case study Jordan. *Energy Convers. Manag.* **2022**, *260*, 115598. [CrossRef]
15. Calero-Lara, M.; López-Luque, R.; Casares, F.J. Methodological Advances in the Design of Photovoltaic Irrigation. *Agronomy* **2021**, *11*, 2313. [CrossRef]
16. Guillén-Arenas, F.J.; Fernández-Ramos, J.; Narvarte, L. A New Strategy for PI Tuning in Photovoltaic Irrigation Systems Based on Simulation of System Voltage Fluctuations Due to Passing Clouds. *Energies* **2022**, *15*, 7191. [CrossRef]
17. Cervera-Gascó, J.; Perea, R.G.; Montero, J.; Moreno, M.A. Prediction Model of Photovoltaic Power in Solar Pumping Systems Based on Artificial Intelligence. *Agronomy* **2022**, *12*, 693. [CrossRef]
18. Fara, L.; Craciunescu, D.; Fara, S. Numerical Modelling and Digitalization Analysis for a Photovoltaic Pumping System Placed in the South of Romania. *Energies* **2021**, *14*, 2778. [CrossRef]
19. Boukebbous, S.E.; Benbaha, N.; Bouchakour, A.; Ammar, H.; Bouhoun, S.; Kerdoun, D. Experimental performance assessment of photovoltaic water pumping system for agricultural irrigation in semi-arid environment of Sebseb—Ghardaia, Algeria. *Int. J. Energy Environ. Eng.* **2022**, *13*, 979–994. [CrossRef]
20. Santra, P. Performance evaluation of solar PV pumping system for providing irrigation through micro-irrigation techniques using surface water resources in hot arid region of India. Agric. *Water Manag.* **2021**, *245*, 106554. [CrossRef]
21. Zhao, B.; Ren, Y.; Gao, D.; Xu, L. Performance ratio prediction of photovoltaic pumping system based on grey clustering and second curvelet neural network. *Energy* **2019**, *171*, 360–371. [CrossRef]
22. Wurthmann, K.A. Designing photovoltaic arrays for groundwater pumping for remote agriculture using synthetically generated daily rainfall and irrigation needs. *J. Eng. Des. Technol.* **2021**. *ahead-of-print*. [CrossRef]
23. García, A.M.; Perea, R.G.; Poyato, E.C.; Barrios, P.M.; Díaz, J.R. Comprehensive sizing methodology of smart photovoltaic irrigation systems. *Agric. Water Manag.* **2020**, *229*, 105888. [CrossRef]
24. Cervera-Gascó, J.; Montero, J.; del Castillo, A.; Tarjuelo, J.M.; Moreno, M.A. EVASOR, an Integrated Model to Manage Complex Irrigation Systems Energized by Photovoltaic Generators. *Agronomy* **2020**, *10*, 331. [CrossRef]
25. Monís, J.I.; López-Luque, R.; Reca, J.; Martínez, J. Multistage Bounded Evolutionary Algorithm to Optimize the Design of Sustainable Photovoltaic (PV) Pumping Irrigation Systems with Storage. *Sustainability* **2020**, *12*, 1026. [CrossRef]
26. Mindú, A.J.; Capece, J.A.; Araújo, R.E.; Oliveira, A.C. Feasibility of Utilizing Photovoltaics for Irrigation Purposes in Moamba, Mozambique. *Sustainability* **2021**, *13*, 10998. [CrossRef]
27. Ghasemi-Mobtaker, H.; Mostashari-Rad, F.; Saber, Z.; Chau, K.-W.; Nabavi-Pelesaraei, A. Application of photovoltaic system to modify energy use, environmental damages and cumulative exergy demand of two irrigation systems—A case study: Barley production of Iran. *Renew. Energy* **2020**, *160*, 1316–1334. [CrossRef]

28. Raza, F.; Tamoor, M.; Miran, S.; Arif, W.; Kiren, T.; Amjad, W.; Hussain, M.I.; Lee, G.-H. The Socio-Economic Impact of Using Photovoltaic (PV) Energy for High-Efficiency Irrigation Systems: A Case Study. *Energies* **2022**, *15*, 1198. [CrossRef]
29. Pombo-Romero, J.; Rúas-Barrosa, O. A Blockchain-Based Financial Instrument for the Decarbonization of Irrigated Agriculture. *Sustainability* **2022**, *14*, 8848. [CrossRef]
30. Lefore, N.; Closas, A.; Schmitter, P. Solar for all: A framework to deliver inclusive and environmentally sustainable solar irrigation for smallholder agriculture. *Energy Policy* **2021**, *154*, 112313. [CrossRef]
31. Chazarra-Zapata, J.; Molina-Martínez, J.M.; de la Cruz, F.-J.P.; Parras-Burgos, D.; Canales, A.R. How to Reduce the Carbon Footprint of an Irrigation Community in the South-East of Spain by Use of Solar Energy. *Energies* **2020**, *13*, 2848. [CrossRef]
32. Maslowaten. Maslowaten H2020 Project. 2016. Available online: http://maslowaten.eu/ (accessed on 1 April 2021).
33. Fernández-Ramos, J.; Narvarte-Fernández, L.; Poza-Saura, F. Improvement of photovoltaic pumping systems based on standard frequency converters by means of programmable logic controllers. *Sol. Energy* **2010**, *84*, 101–109. [CrossRef]
34. Almeida, R.H.; Carrêlo, I.B.; Lorenzo, E.; Narvarte, L.; Fernández-Ramos, J.; Martínez-Moreno, F.; Carrasco, L.M. Development and Test of Solutions to Enlarge the Power of PV Irrigation and Application to a 140 kW PV-Diesel Representative Case. *Energies* **2018**, *11*, 3538. [CrossRef]
35. Todde, G.; Murgia, L.; Deligios, P.A.; Hogan, R.; Carrelo, I.; Moreira, M.; Pazzona, A.; Ledda, L.; Narvarte, L. Energy and environmental performances of hybrid photovoltaic irrigation systems in Mediterranean intensive and super-intensive olive orchards. *Sci. Total. Environ.* **2019**, *651*, 2514–2523. [CrossRef]
36. Das, M.; Mandal, R. A comparative performance analysis of direct, with battery, supercapacitor, and battery-supercapacitor enabled photovoltaic water pumping systems using centrifugal pump. *Sol. Energy* **2018**, *171*, 302–309. [CrossRef]
37. Luque, A.; Hegedus, S. *Handbook of Photovoltaic Science and Engineering*, 2nd ed.; Johm Wiley & Sons: Chichester, UK, 2011.
38. Herraiz, J.I.; Fernández-Ramos, J.; Almeida, R.H.; Báguena, E.M.; Castillo-Cagigal, M.; Narvarte, L. On the tuning and performance of Stand-Alone Large-Power PV irrigation systems. *Energy Convers. Manag.* **2022**, *13*, 100175. [CrossRef]
39. Livera, A.; Theristis, M.; Koumpli, E.; Theocharides, S.; Makrides, G.; Sutterlueti, J.; Stein, J.S.; Georghiou, G.E. Data processing and quality verification for improved photovoltaic performance and reliability analytics. *Prog. Photovolt. Res. Appl.* **2021**, *29*, 143–158. [CrossRef]
40. Koumpli, E. Impact of Data Quality on Photovoltaic (PV) Performance Assessment. 2017. Available online: https://repository.lboro.ac.uk/articles/thesis/Impact_of_data_quality_on_photovoltaic_PV_performance_assessment/9534902 (accessed on 12 February 2023).
41. Lindig, S.; Louwen, A.; Moser, D.; Topic, M. Outdoor PV System Monitoring—Input Data Quality, Data Imputation and Filtering Approaches. *Energies* **2020**, *13*, 5099. [CrossRef]
42. IEC. *IEC 61724-2 TS: Photovoltaic System Performance—Part 2: Capacity Evaluation Method*; IEC: Vienna, Austria, 2016.